Supplementary Information

Figure S1. Analytical size exclusion chromatography with FBP21$^{200-376}$ and Brr2^{FL}, Brr2^{HR}, Brr2^{NC} and Brr2^{CC}.

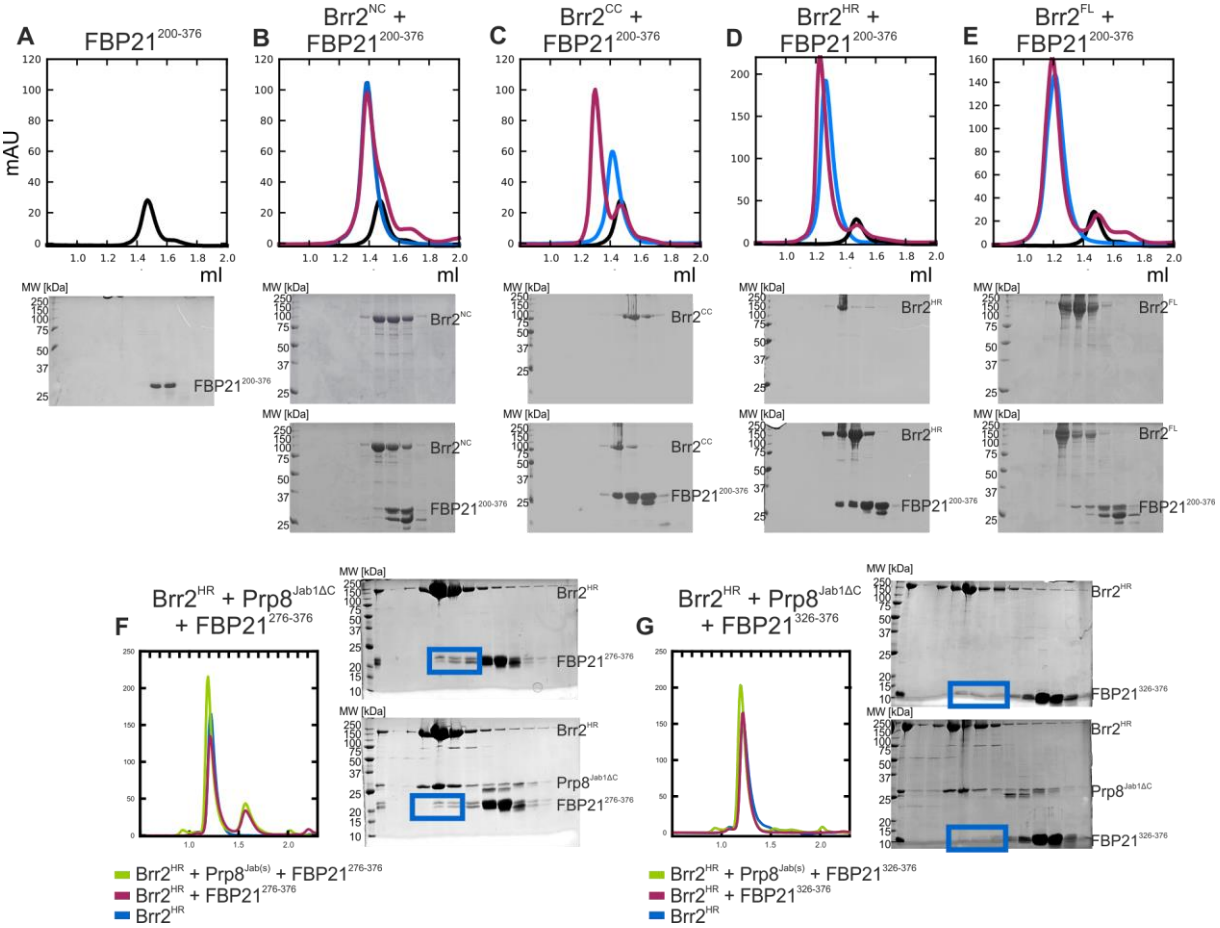

A-E) Analytical size exclusion chromatography experiments show the interaction between FBP21$^{200-376}$ and Brr2. The chromatograms show the UV-absorption at 280 nm of FBP21 alone (black), Brr2 construct alone (blue) and the complex (pink). The gel in (A) contains the fractions of FBP21 alone. The top gels in B-E contain the fractions of the Brr2 construct alone; the bottom gel contains the fractions of the complex. The additional band below FBP21 is a degradation product that could not be separated in preparative size exclusion chromatography. F-G) Analytical size exclusion chromatography experiments show the interaction between FBP21$^{276-376}$ (F) or FBP21$^{326-376}$ (G), Brr2^{HR} and Prp8$^{Jab1\Delta C}$. The chromatograms show the UV-absorption at 280 nm of FBP21 alone (black), Brr2^{HR} in complex with FBP21 (pink) and the complex of all three proteins (green). The top gels in F-G contain the fractions of Brr2^{HR} in complex with FBP21; the bottom gel contains the fractions of the trimeric complex. Blue boxes indicate the band corresponding to FBP21 fragments or absence thereof.

Figure S2. Selectively labeled ^{1}H-^{15}N-TROSY-HSQCs

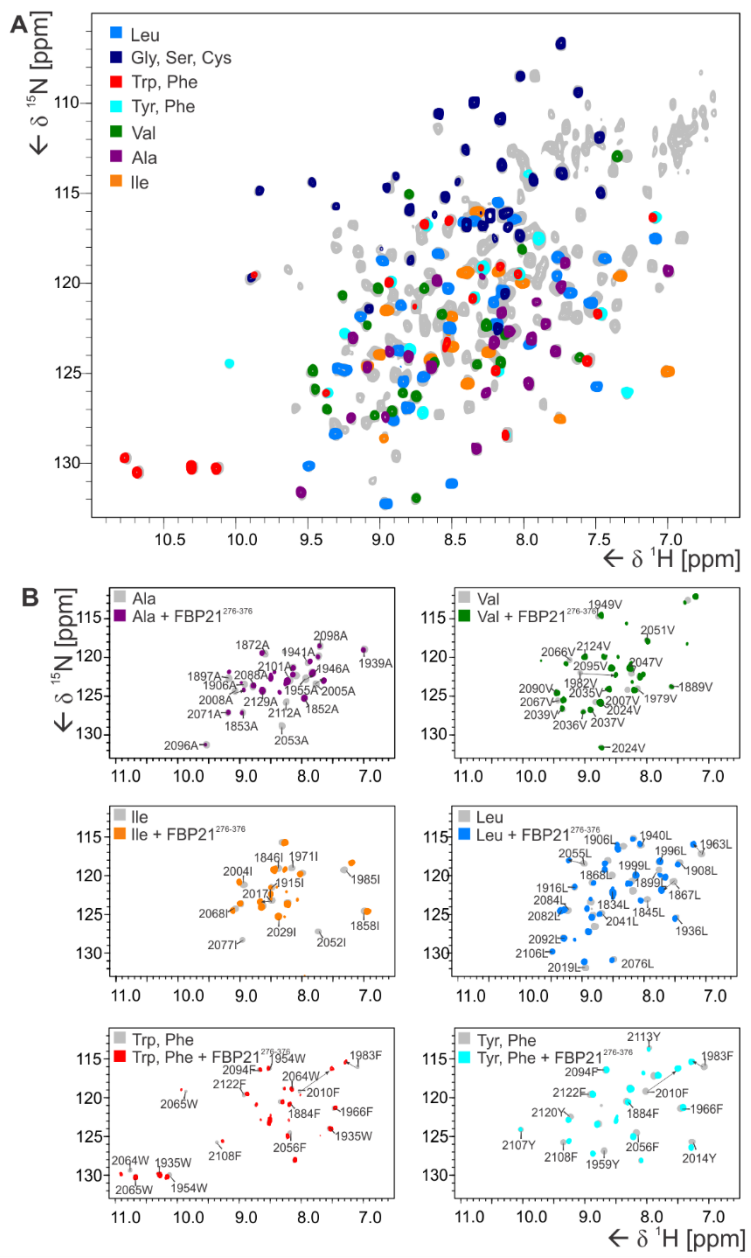

The assignment of Brr2$^{C\text{-}Sec63}$ was aided amino acid type-selectively labeled Brr2$^{C\text{-}Sec63}$. ^{1}H-^{15}N-TROSY-HSQC spectra were recorded with the selectively labeled Brr2$^{C\text{-}Sec63}$ alone (A) and in complex with FBP21$^{276\text{-}376}$ (B). In a, the grey spectrum corresponds to uniformly ^{15}N-labeled Brr2$^{C\text{-}Sec63}$. Each of the amino acid types used for selective labeling is shown in a different color. In B, the grey spectrum corresponds to the selectively labeled Brr2$^{C\text{-}Sec63}$ and the colored spectrum to the selectively labeled Brr2$^{C\text{-}Sec63}$ in complex with FBP21$^{276\text{-}376}$. Assigned peaks are labeled with their corresponding residue name.

Figure S3. NMR titration experiment with ^{15}N-labeled Brr2$^{C\text{-}Sec63}$ and FBP21$^{276\text{-}376}$.

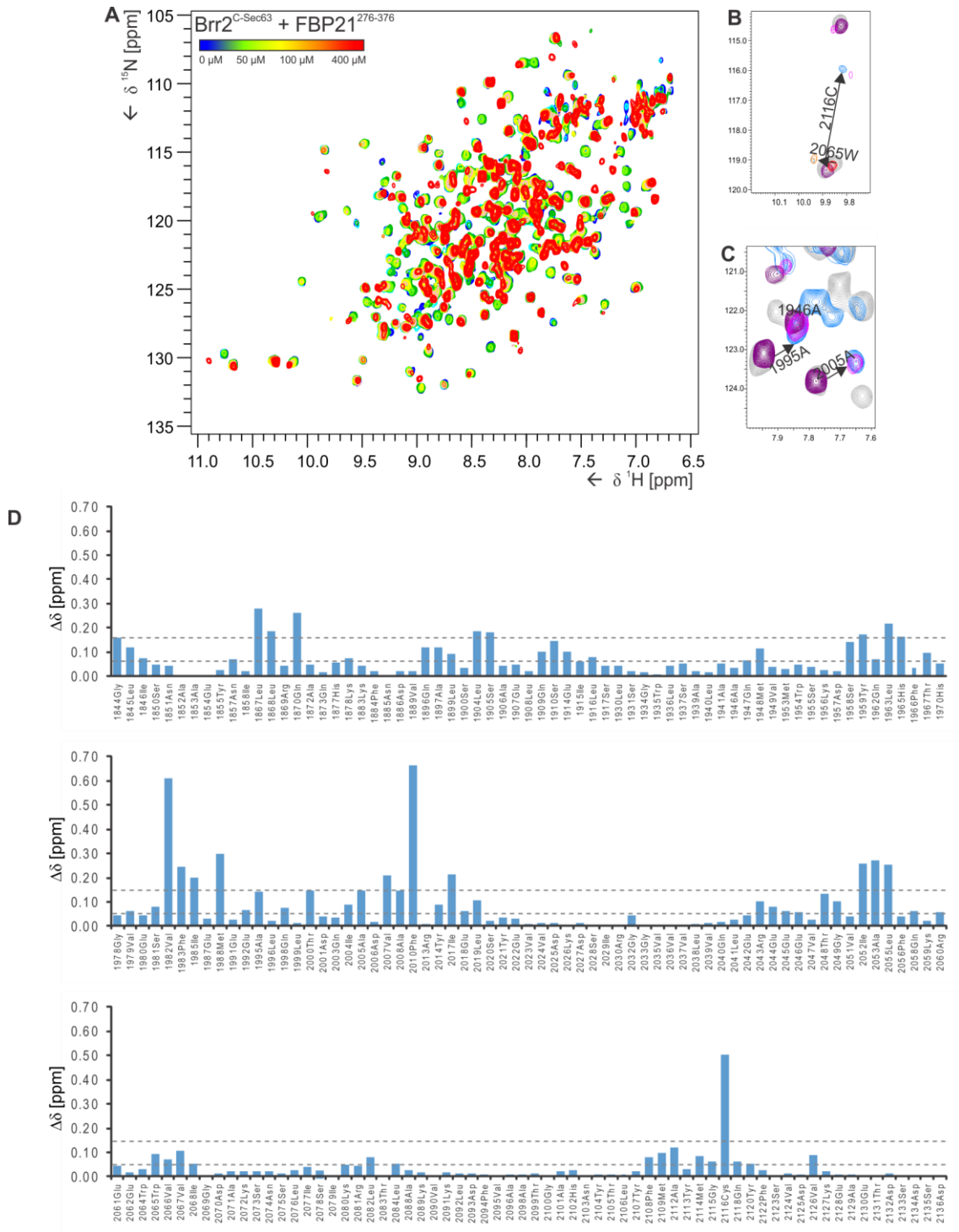

A) The NMR titration experiment with FBP21$^{276\text{-}376}$ shows concentration dependent chemical shift changes. The interaction is in the intermediate exchange regime, with line broadening of most peaks at intermediate ligand concentrations and reappearance of peaks at high ligand concentrations. B+C) In many cases, the identification of the resonances in the complex was difficult and could only be achieved through selectively labeled Brr2$^{C\text{-}Sec63}$. This was further

complicated by some peaks covering very long chemical shift distances (shown is the example of 2116C). D) Chemical shift differences of each residue upon the addition of 400 µM FBP21$^{276-376}$. The dotted lines indicate the average chemical shift difference and the average chemical shift difference plus the standard deviation. For mapping the residues on the structure of Brr2$^{C-Sec63}$ (Figure 2C), all residues with a chemical shift distance larger than the average chemical shift distance (Δδ =0.066 ppm) were considered to be shifting (pink) and all residues with a chemical shift distance larger than the average chemical shift distance plus standard deviation (Δδ =0.156 ppm) were considered to be shifting strongly (dark pink).

Figure S4. Supplementary NMR experiments

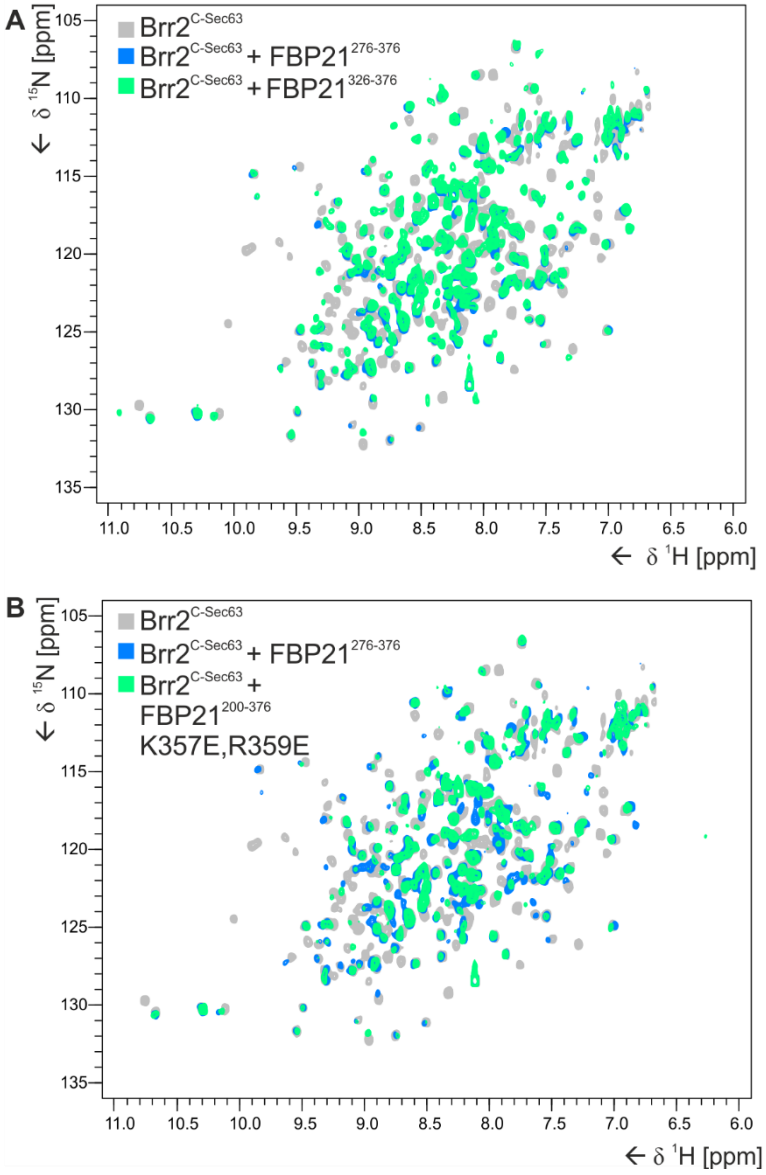

A) Overlay of ^{1}H-^{15}N-TROSY-HSQC spectra of 100 µM Brr2$^{C\text{-}Sec63}$ alone (gray), Brr2$^{C\text{-}Sec63}$ in presence of 200 µM FBP21$^{276\text{-}376}$ (blue) and Brr2$^{C\text{-}Sec63}$ in presence of 400 µM FBP21$^{326\text{-}376}$ (green). Binding of FBP21$^{276\text{-}376}$ and FBP21$^{326\text{-}376}$ induced similar chemical shift changes. B) Overlay of ^{1}H-^{15}N-TROSY-HSQC spectra of 100 µM Brr2$^{C\text{-}Sec63}$ alone (gray), Brr2$^{C\text{-}Sec63}$ with FBP21$^{276\text{-}376}$ (blue) and Brr2$^{C\text{-}Sec63}$ with 200 µM FBP21$^{200\text{-}376}$ K357E R359E (green).

Figure S5: Signal intensities in presence of the paramagnetic enhancer Gd(DPTA)$^{2-}$

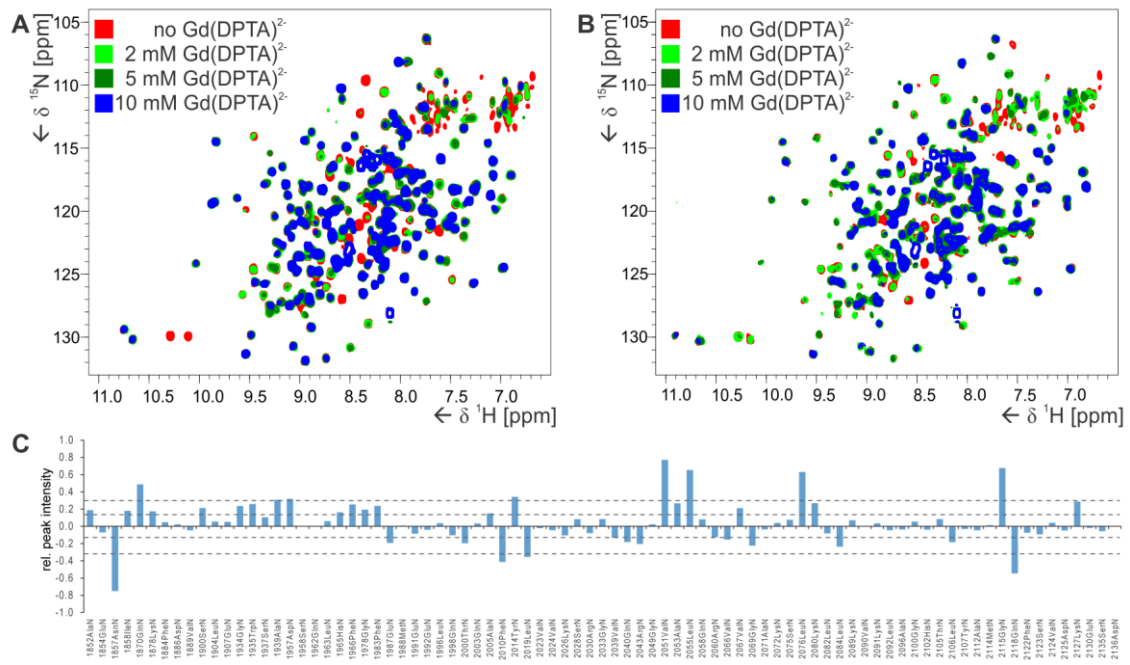

A) Spectrum of Brr2$^{C\text{-}Sec63}$ in presence of 0 mM (red), 2 mM (light green), 5 mM (dark green) or 10 mM (blue) Gd(DTPA)$^{2-}$. B) Spectrum of Brr2$^{C\text{-}Sec63}$ in complex with FBP21$^{276\text{-}376}$ in presence of 0 mM (red), 2 mM (light green), 5 mM (dark green) or 10 mM (blue) Gd(DTPA)$^{2-}$. C) Residue-by-residue analysis of differential effects of Gd(DTPA)$^{2-}$ in presence or absence of FBP21 (mapped on the structure in Figure 2D). Residues were considered to be protected or de-protected when the signal intensity loss was larger than the average difference (Δ=0.16), residues were considered to be strongly protected or de-protected when the signal intensity loss difference was larger than the average difference plus standard deviation (Δ=0.33).

Figure S6. ITC measurements.

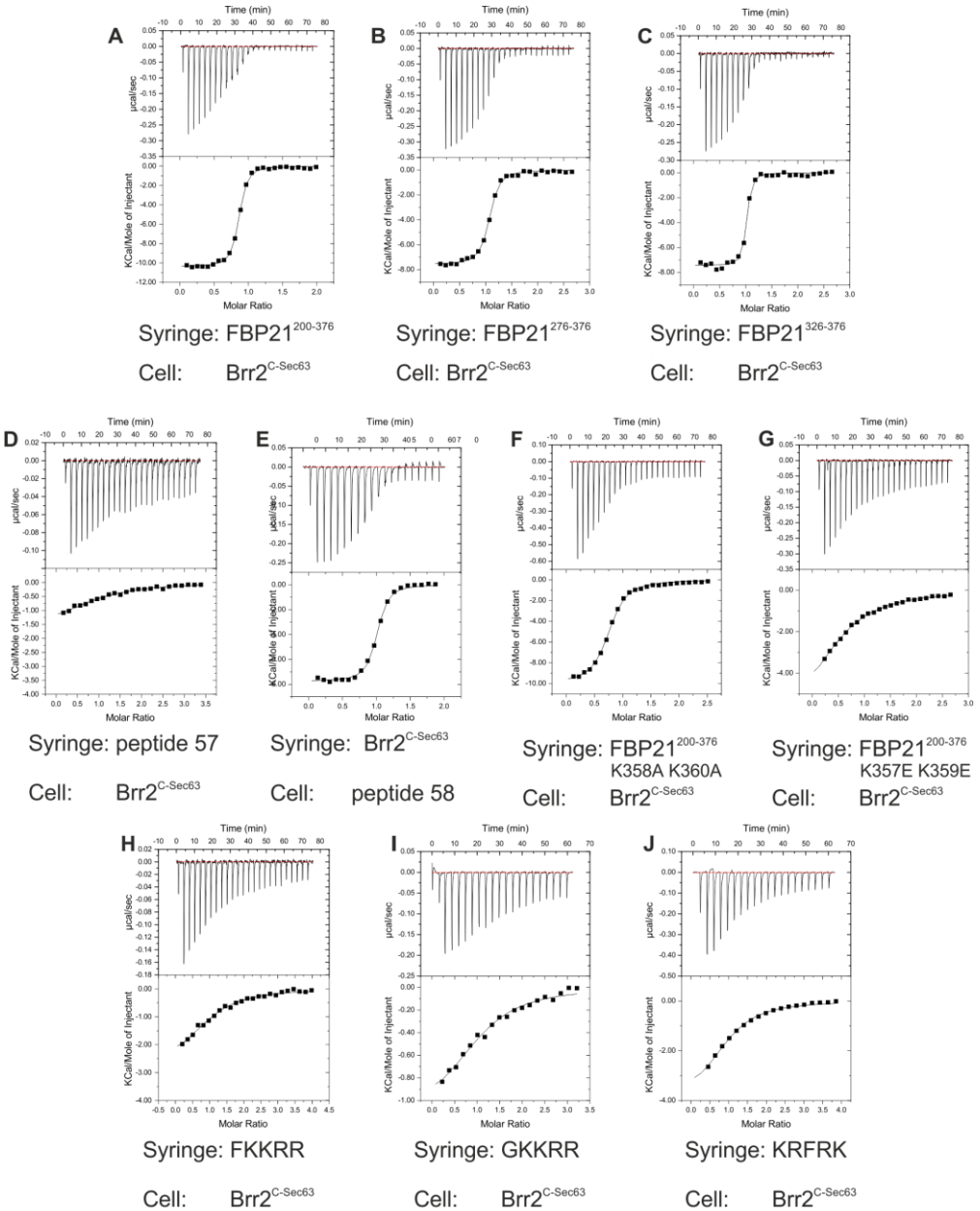

K

Ligand	K_D [µM]	N	ΔH [kcal/mol]	ΔS [cal/mol/K]
FBP21$^{200-376}$	0.13 ± 0.004	0.81 ± 0.03	-10.73 ± 0.29	-4.42 ± 1.05
FBP21$^{276-376}$	0.30 ± 0.05	1.05 ± 0.01	-7.70 ± 0.13	4.07 ± 0.74
FBP21$^{326-376}$	0.11 ± 0.001	0.98 ± 0.01	-7.44 ± 0.24	7.31 ± 0.92
peptide 57	27.5 ± 2.21	1.10 ± 0.16	-1.87 ± 0.09	14.60 ± 1.16
peptide 58	1.34 ± 0.19	0.99 ± 0.02	-9.91 ± 0.65	-6.33 ± 2.40
FKKRR	19.97 ± 1.15	1.01 ± 0.07	- 3.12 ± 0.15	11.07 ± 0.52
GKKRR	36.95 ± 5.99	1.11 ± 0.07	-1.27 ± 0.09	16.07 ± 0.45
KRFRK	27.29 ± 3.01	0.99 ± 0.04	-3.79 ± 0.18	8.18 ± 0.68
FBP21$^{200-376}$ K358A R360A	2.13 ± 0.37	0.76 ± 0.01	-10.51 ± 0.50	-3.77 ± 2.03
FBP21$^{200-376}$ K357E R359E	27.88 ± 0.93	0.69 ± 0.09	- 7.34 ± 0.34	-9.27 ± 1.19

A-J) ITC raw data of Brr2 $^{C\text{-}Sec63}$ and (A) FBP21$^{200\text{-}376}$, (B) FBP21$^{276\text{-}376}$, (C) FBP21$^{326\text{-}376}$, (D) peptide 57, (E) peptide 58, (F) FBP21$^{200\text{-}376}$ K358A R360A and (G) FBP21$^{200\text{-}376}$ K357E R359E. (H) peptide FKKRR, (I) peptide GKKRR, (J) peptide KRFRK. K) Thermodynamic data derived from ITC measurements. All experiments were performed in triplicates.

Figure S7: Chemical shift changes with Peptide 57 and Peptide 58

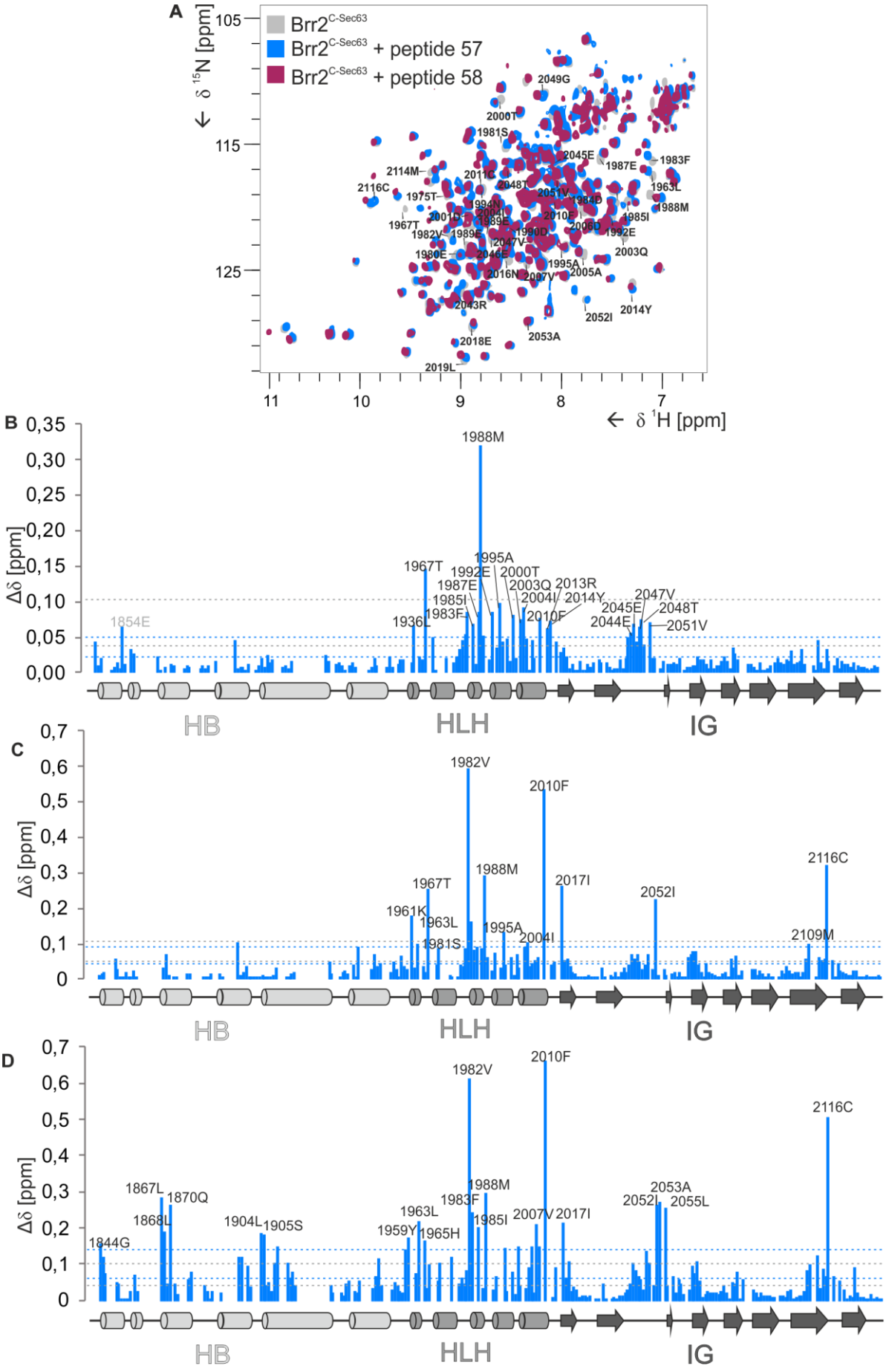

A) Overlay of ^{1}H-^{15}N-TROSY-HSQC spectra of Brr2$^{C\text{-}Sec63}$ (gray), Brr2$^{C\text{-}Sec63}$ in presence of a sevenfold excess of peptide 57 and Brr2$^{C\text{-}Sec63}$ in presence of a sevenfold excess of peptide 58 (dark pink). Assigned shifting resonances are annotated. B) Chemical shift differences of each residue upon the addition of 700 µM peptide 57. The blue dotted lines indicate the average chemical shift distance and the average chemical shift distance plus the standard deviation of this experiment and were used as thresholds for mapping the residues showing chemical shift changes on the structure of Brr2$^{C\text{-}Sec63}$ (Figure 3D). All residues with a chemical shift distance larger than the average chemical shift distance (Δδ=0.022 ppm) were considered to be shifting (pink) and all residues with a chemical shift distance larger than the average chemical shift distance plus standard deviation (Δδ =0.052 ppm) were considered to be shifting strongly (dark pink). The gray dotted lines indicate the average chemical shift distance and the average chemical shift distance plus the standard deviation of all experiments shown here and were used to compare binding sites on Brr2$^{C\text{-}Sec63}$ (Figure S8). The overall average chemical shift change was Δδ =0.042 ppm and the overall average chemical shift change plus standard deviation was Δδ =0.113 ppm. C) Chemical shift distances of each residue upon the addition of 700 µM peptide 58. The blue dotted lines indicate the average chemical shift difference (Δδ=0.040 ppm) and the average chemical shift distance plus standard deviation (Δδ =0.109 ppm) of this experiment, the gray dotted lines the global average and average plus standard deviation. D) Chemical shift differences of each residue upon the addition of 400 µM FBP21$^{276\text{-}376}$. The blue dotted lines indicate the average chemical shift difference (Δδ=0.066 ppm) and the average chemical shift distance plus standard deviation (Δδ=0.156 ppm) of this experiment, the gray dotted lines the global average and average plus standard deviation.

Figure S8. Charge plot Brr2$^{C\text{-}Sec63}$ and binding sites of the positively charged Peptide 57 and FBP21$^{276\text{-}376}$

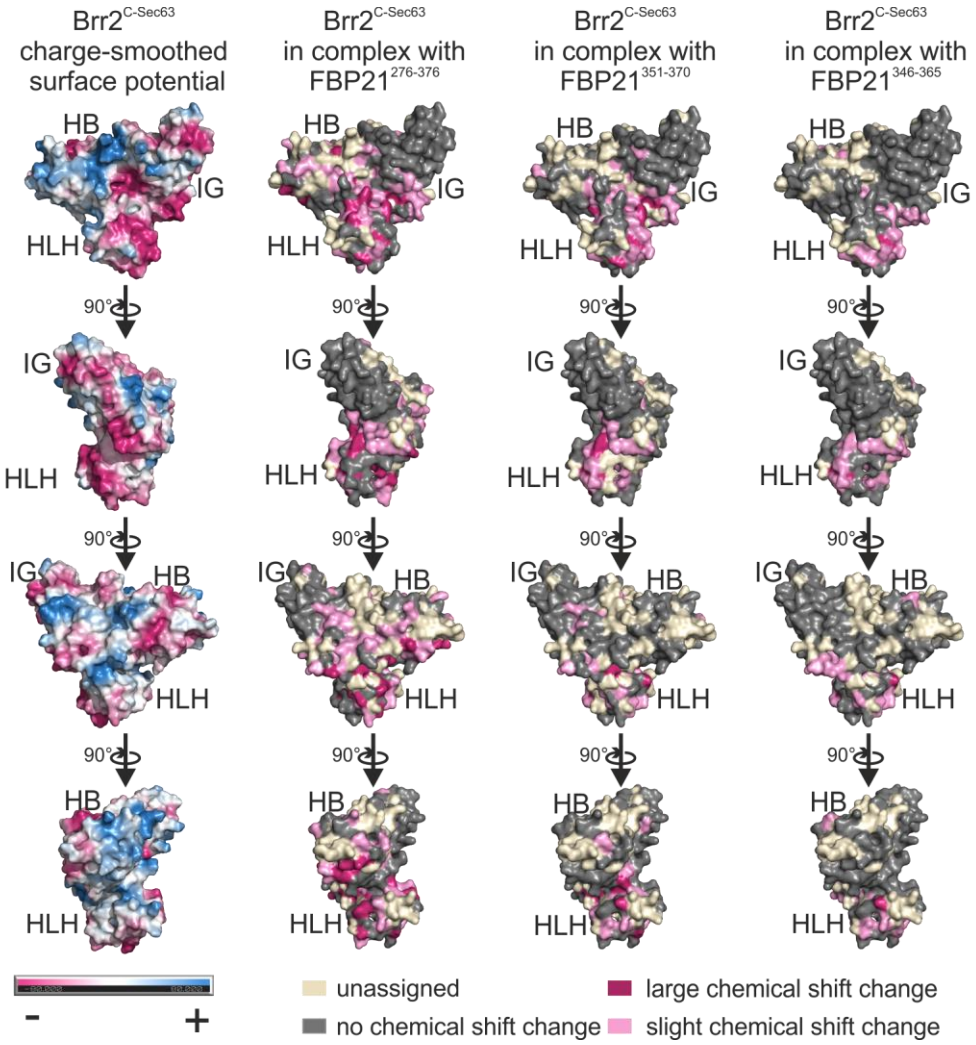

Side-by-side comparison of the residues exhibiting chemical shift changes with FBP21$^{276\text{-}376}$, the residues exhibiting chemical shift changes upon interaction with peptide 58, the residues showing chemical shift changes upon interaction with peptide 57 and the charge-smoothed electrostatic potential (generated using PyMol) of Brr2$^{C\text{-}Sec63}$. To improve comparison, a global threshold was defined by the global average and standard deviation to identify residues showing strong chemical shift changes ($\Delta\delta > 0.113$ ppm) and weaker chemical shift changes ($\Delta\delta = 0.042$ ppm).

Figure S9. Electrophoretic mobility shift assay experiments

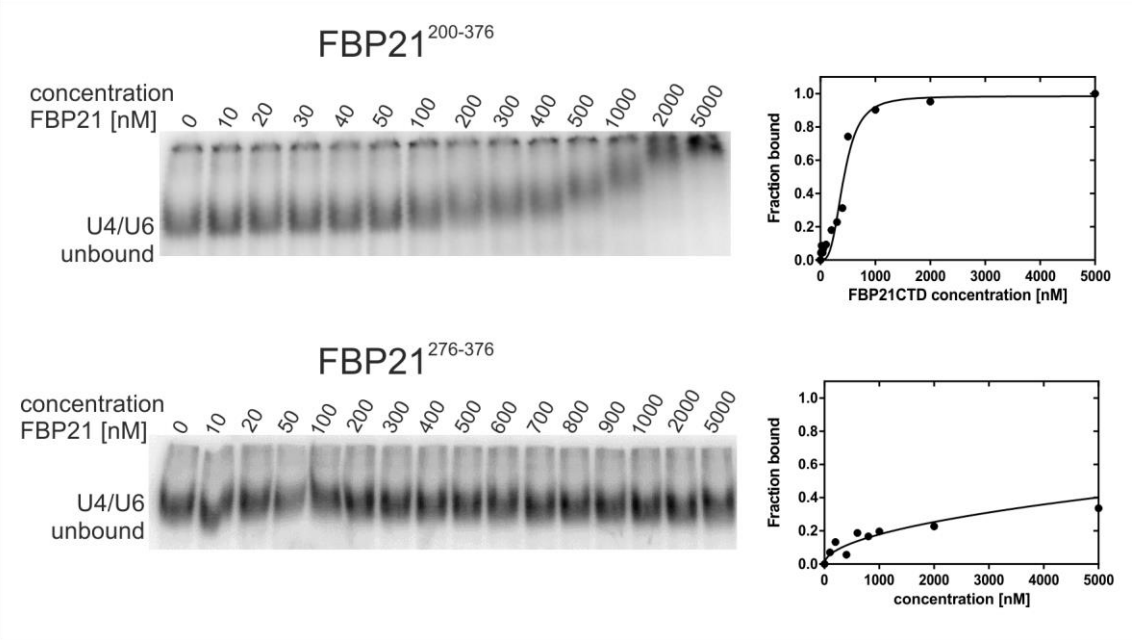

Electrophoretic mobility shift assays of U4/U6 di-snRNA in presence of increasing concentrations of FBP21$^{200-376}$ or FBP21$^{276-376}$, respectively, showed that while FBP21 interacts with U4/U6 di-snRNA, FBP21$^{276-376}$ does not. Shown are raw data (left) and the fraction bound at each concentration.

Figure S10. Concentration-dependent inhibition of Brr2^{HR} helicase activity by FBP21$^{200-376}$ and FBP21$^{276-376}$

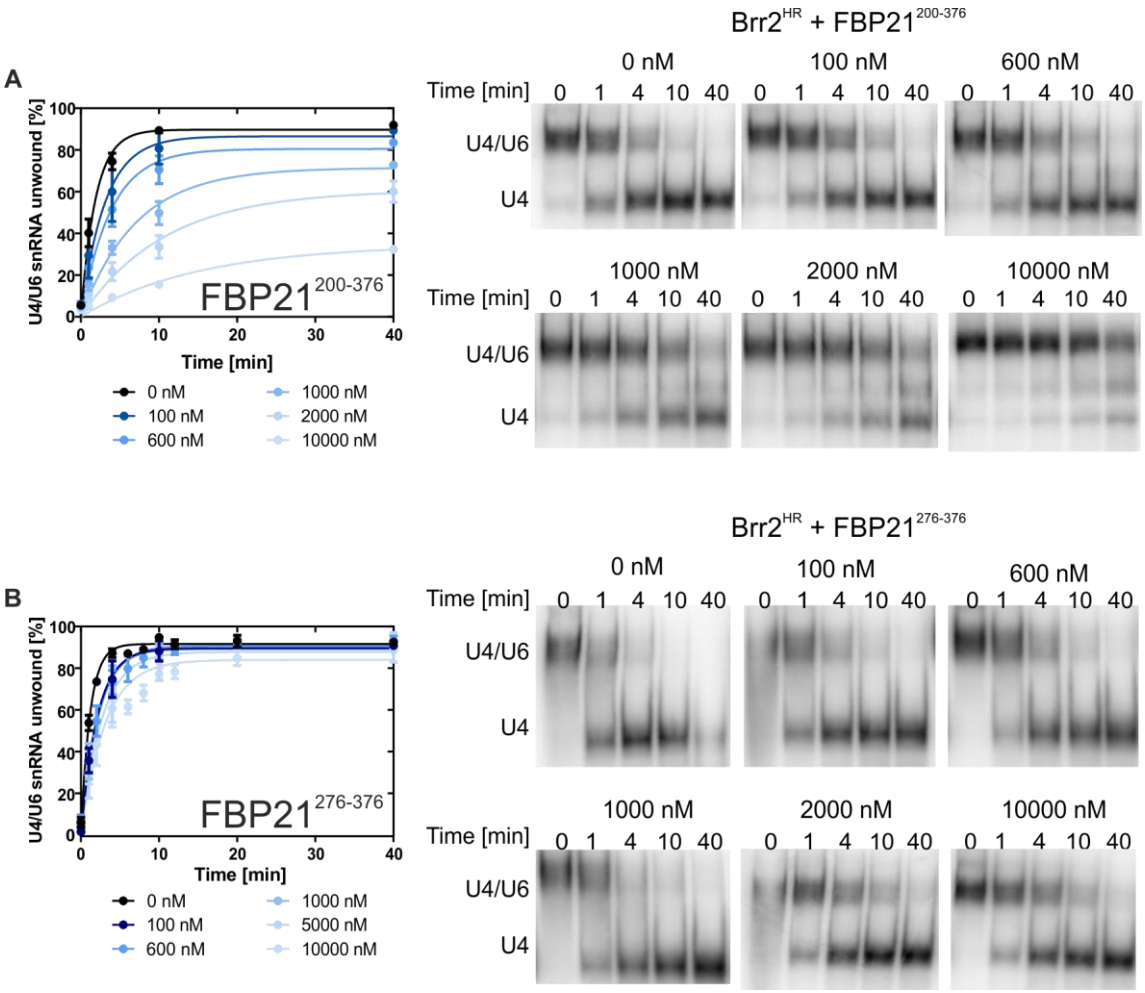

A) Quantification and representative native gels of the U4/U6 di-snRNA unwinding by Brr2^{HR} in presence of various concentrations of FBP21$^{200-376}$. All points were taken at least in triplicates. B) Quantification and representative native gels of the U4/U6 di-snRNA unwinding by Brr2^{HR} in presence of various concentrations of FBP21$^{276-376}$. All points were taken at least in triplicates.

Figure S11. FBP21, Brr2$^{C\text{-}Sec63}$ and SmB

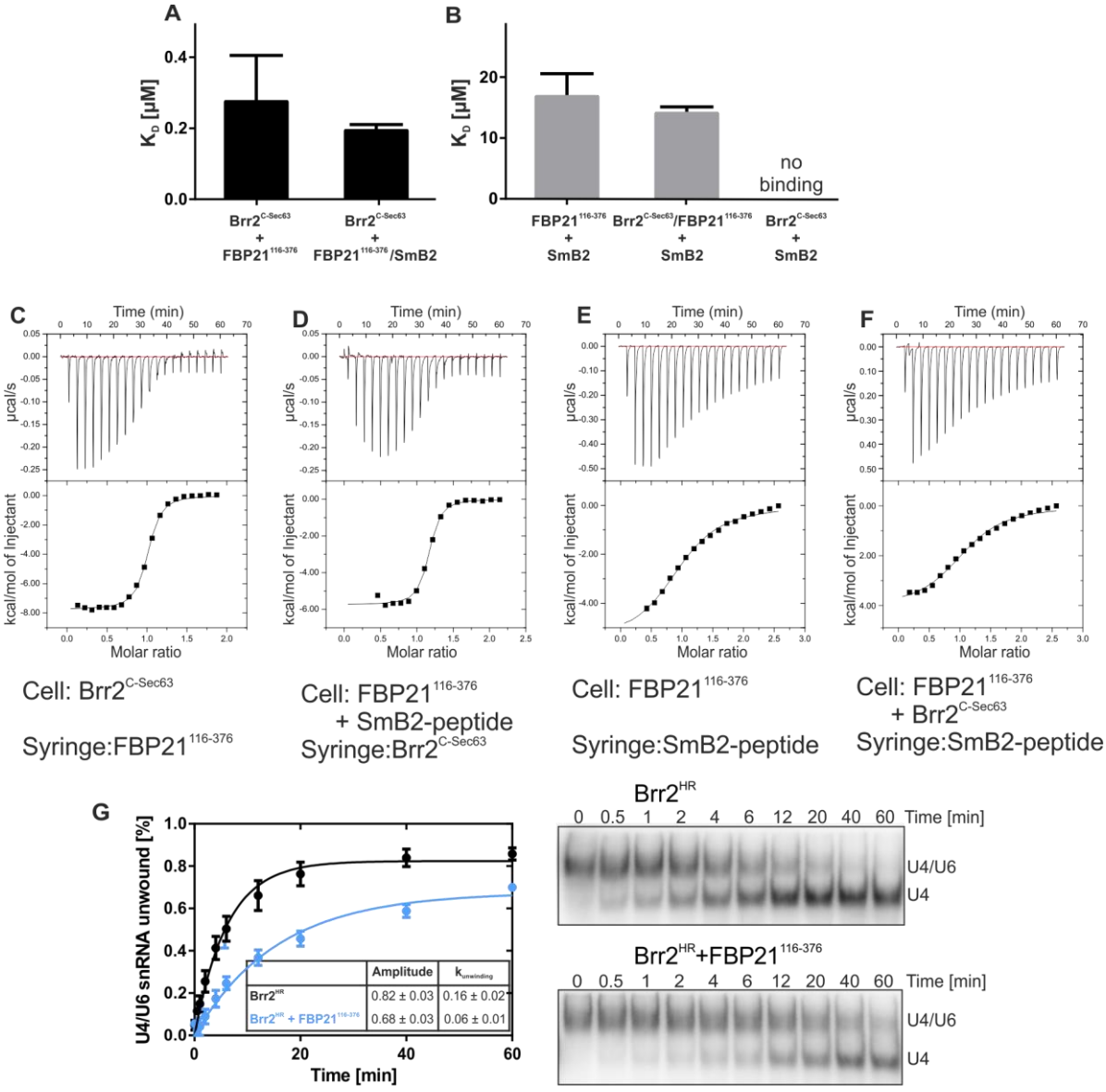

FBP21$^{116\text{-}376}$ interacts independently with SmB-peptide and Brr2$^{C\text{-}Sec63}$. A) Dissociation constants of the interaction between Brr2$^{C\text{-}Sec63}$ and FBP21$^{116\text{-}376}$ in absence or presence of SmB-peptide. B) Dissociation constants of FBP21$^{116\text{-}376}$ and SmB-peptide in presence or absence of Brr2$^{C\text{-}Sec63}$. C-F) Exemplary ITC curves of the interactions of C) Brr2$^{C\text{-}Sec63}$ with FBP21$^{116\text{-}376}$, D) Pre-incubated FBP21$^{116\text{-}376}$ and SmB-peptide and Brr2$^{C\text{-}Sec63}$ E) FBP21$^{116\text{-}376}$ and SmB-peptide, F) Pre-incubated FBP21$^{116\text{-}376}$ and Brr2$^{C\text{-}Sec63}$ with SmB-peptide and G) Brr2$^{C\text{-}Sec63}$ with SmB-peptide. H) Unwinding assay with Brr2^{HR} in presence or absence of FBP21$^{116\text{-}376}$.